TerraTek Core Services, Inc.®

PETROGRAPHIC EVALUATION

of Four Samples From the
Baca Geothermal Area,
Valles Caldera, New Mexico
for
University of Utah Research Institute
TTCS File No. 630

• 360 Wakara Way • Salt Lake City, Utah 84108 • (801) 584-2480
• 920 Central Avenue • Suite #2 • Billings, Montana 59102 • (406) 256-0371
• 1625 Broadway • Suite 2110 • Denver, Colorado 80220 • (303) 595-0263

INTRODUCTION

Four (4) air drilled samples were selected for petrographic evaluation from the Baca-20 well in the Baca Geothermal Area, Valles Caldera, New Mexico. The petrographic analysis consisted of scanning electron microscopy (SEM) to aid in the determination of framework grains, the distribution of clays and pore space.

The four samples are from various depths of the Baca-20 well which passes through Pleistocene and Pliocene rhyolite ash flow tuffs and other, more intermediate, volcanic rocks. Hulen and Nielson (1982) consider that the stratigraphic horizons which samples 3196 and 2460 represent are aquifers which partially control thermal fluid migration. Samples 560 and 360 are from the densely welded, yet highly altered rhyolite tuff. Detailed descriptions of these samples are given below. More comprehensive mineralogic and general geologic investigations have been done by Hulen and Nielson (1982 and 1983) and Smith and Bailey (1968). Readers should refer to these papers for a better understanding of the complete geothermal system.

TEXTURE & MINERALOGY

Sample 3196 (taken from the interval between 3196 and 3216') is a lower medium-grained sublitharenite chiefly composed of moderately sorted subangular volcanic clasts. The major components are quartz and feldspar with minor occurrences of pyrite. The moderate sorting and subangular nature of this sample is indicative of a submature sandstone. In addition, two authigenic clays, illite and chlorite, are recognizable. The illite takes on a massive form, whereas the chlorite is bladed and found bridging pore space. Further reduction of primary porosity can be attributed to both compaction due to overburden and extensive quartz overgrowths. The remaining intergranular porosity and intragranular porosity is the result of partial dissolution of clay and framework grains at the grain boundaries.

Sample 2460 (taken from the interval between 2460 and 2474') is an altered, finely cellular pumice. The pumice is almost completely

altered to illite with possible glass shard ghosts and rare molds of phenocrysts that rested in the pumaceous matrix. Micrographs show evidence of leached phenocrysts which formed during cooling and have been secondarily leached, possibly by hydrothermal fluids. The glassy texture of the sample, glass shard ghosts, and cellular nature of the sample are all indicative of pumice origin. This probably represents a minor cooling break in the Tshirege Member, according to Hulen and Nielson (1983).

Sample 560 (taken from interval 560-580') is a siliceous rhyolitic tuff characterized by quartz and feldspar crystals resting in an equally siliceous, finely crystalline groundmass. Other components include biotite, pyrite, and possibly some plagioclase. The quartz is pink to clear and occurs mostly as large euhedral phenocrysts. The pyrite is euhedral and commonly occurs in small veinlets approximately 1mm wide. It is believed by the author that the samples are derived from a rhyolitic ash flow tuff.

Sample 360 (taken from interval 360-380') is a siliceous rhyolite distinguished by euhedral quartz and potassium feldspar phenocrysts. A variety of other minerals exist including plagioclase and pyrite. Pyrite is a minor constituent (<1%) and characteristically has a cubic habit. The pyrite is randomly scattered throughout the sample and is smaller than .1mm in hand specimens. Potassium feldspar has been altered to authigenic clay and these crystals commonly are rimmed by an iron oxide stain imparting, locally, a reddish-brown color to the rock. This sample is also a rhyolite ash flow tuff.

SUMMARY

Of the four samples investigated, three distinct depositional events are represented. Sample 3196, the lower medium-grained sublitharenite, is a moderately sorted subangular sand which was deposited by a fluvial system carrying the clastic debris not far from its source. After deposition the sand has undergone several stages of diagenesis which have greatly reduced the primary porosity and permeability. Reduction of porosity and permeability is primarily due to compaction after burial, the formation of clays (chlorite, illite & illite-smectite) and quartz overgrowths filling intergranular voids. Minor amounts of porosity are associated with secondary partial dissolution of unstable clasts and microporosity associated with the various clay types.

Sample 2460 is believed to be an altered pumice. Although no direct evidence is available, the indirect evidence, glass shard ghosts, euhedral phenocryst molds, and uniformity of cellular-type pores, could be considered characteristic of air-fall pumice. The sample has been altered mostly to a siliceous illite clay according to Hulen 1984 (pers. comm.).

Samples 560 and 360 are mineralogically and texturally similar. Both are rhyolitic tuffs consisting of relatively large phenocrysts of quartz and feldspar resting in a highly siliceous groundmass. Sample 560 had a greater amount of pyrite occurring both as veinlets, consisting of large cubic phenocrysts, and fine disseminated cubic crystals. The beds represented by these samples of densely welded tuffs are unlikely to have primary porosity and permeability, thus permeability would be restricted to fractured areas.

SAMPLE 3196

A. General view of fabric and distribution of moderately sorted framework grains. Chlorite and illite clays commonly coat the grain boundaries infilling porosity. Authigenic quartz overgrowths are also abundant and further decrease porosity. Reduction of primary porosity can be attributed to compaction and the growth of clay and quartz overgrowths. Box outlines area of next micrograph.
X-90

B. Detail view of fabric showing both illite (i) and chlorite (ch) clays and the abundant microporosity associated with them. Authigenic quartz overgrowths extend into the pore and partly occlude the pore throats.
X-2000

C. Overview of fabric of medium-grained sublitharenite showing degree of sorting and roundness. Note the lack of effective porosity. Reduction of porosity is the result of several diagenetic phases: compaction, clay development and quartz overgrowths.
X-50

D. General view of fabric showing distribution of framework grains and the lack of effective porosity. Some secondary intergranular porosity (arrows) has been created by partial dissolution of cement. The following micrograph shows detail of pore.
X-50

SAMPLE 3196

E. Detail view of pore throat lined with quartz overgrowths (arrows) and minor detectable clay. Porosity appears poorly connected and flow of hydrothermal fluids through this zone may further reduce permeability by creating gelatinous precipitate when in contact with the chlorite clay.
X-1200

F. Detail of texture of illite and chlorite clays commonly coating grains and found infilling intergranular porosity. Note the abundant microporosity associated with the clays. This view shows chlorite most abundant with illite as small fibers emanating from chlorite platelets.
X-5000

SAMPLE 2460

A. General view of fabric of an altered pumaceous tuff. The uniformly cellular texture and mineralogy are suspiciously similar to pumice, but the sample's alteration to illite inhibits definite proof.
X-250

B. Detail of fabric of the pumice showing illite replacing a more siliceous parent material. These could be ghosts of previous glass shards.
X-5000

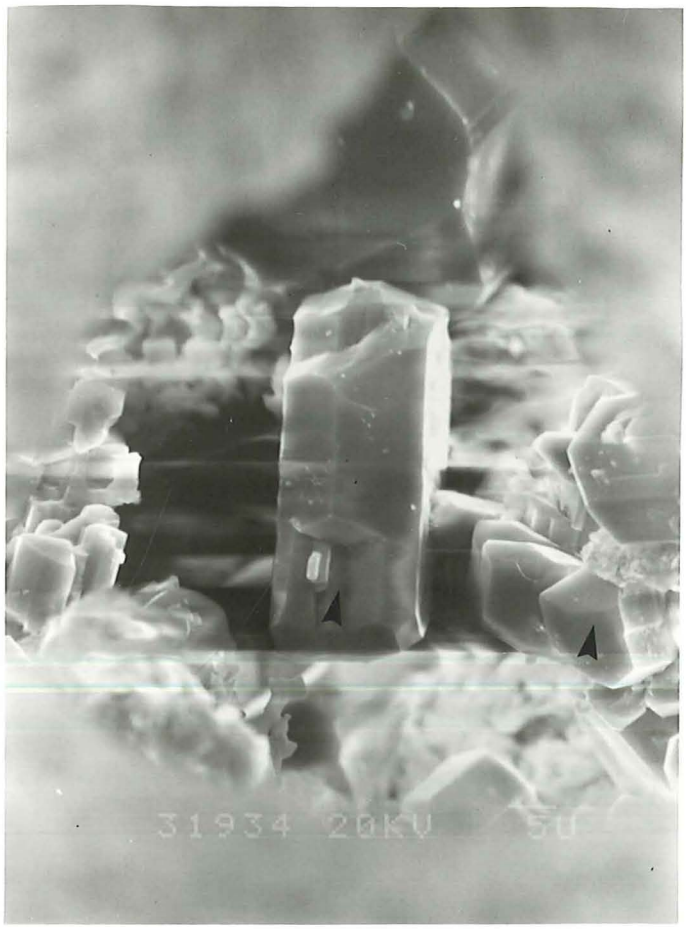

E

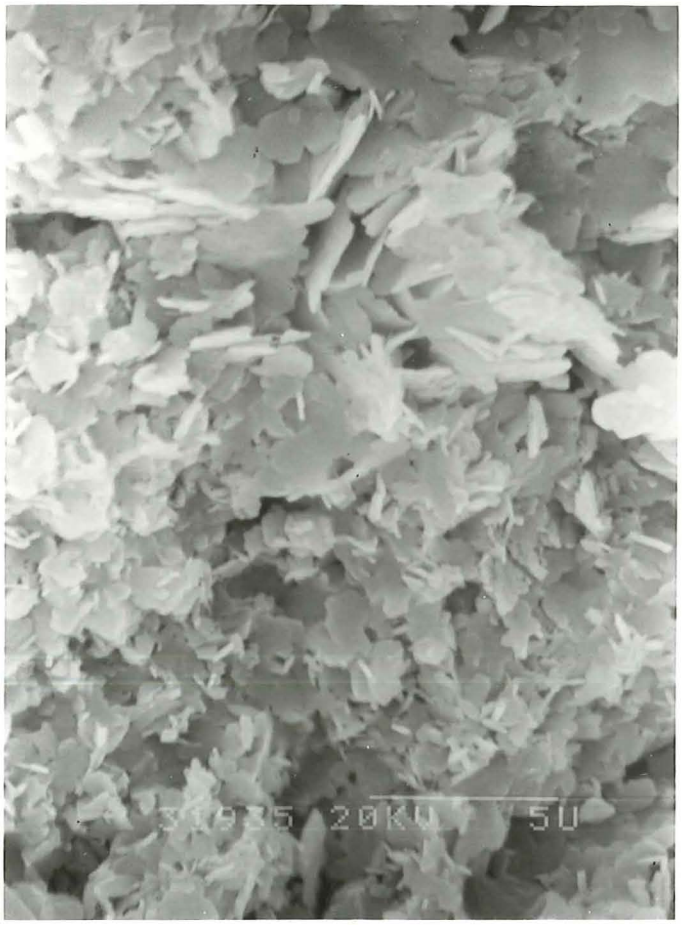

F

A

B

SAMPLE 2460

C. Overview of fabric of pumice showing its cellular nature. Note the leaching of a euhedral phenocryst from the pumice matrix. Kevex elemental analysis shows an abundance of aluminum (Al), silicon (Si) and potassium (K). X-250

D. General view of fabric showing a relatively homogeneous mineralogy and texture. Note the detailed network of pores associated with the clay which comprises most of the sample. X-500

E. Detail of fabric showing poorly crystalline illite and its texture. Note the microporosity associated with the clay. The tortuosity of the pore system is probably extensive; therefore, permeabilities are likely to be lower than expected. X-5000

F. Detail of fabric of pumaceous tuff showing platey nature of clay. Mineralogically the sample is homogeneous. Elemental analysis shows peaks of Al, Si, K and some Fe. X-3500

C

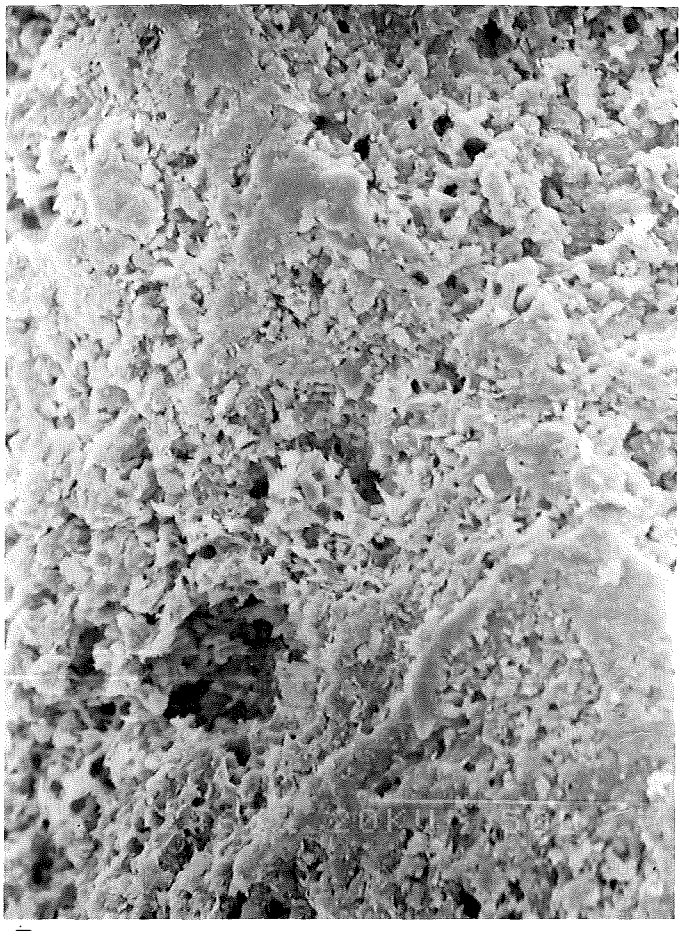

D

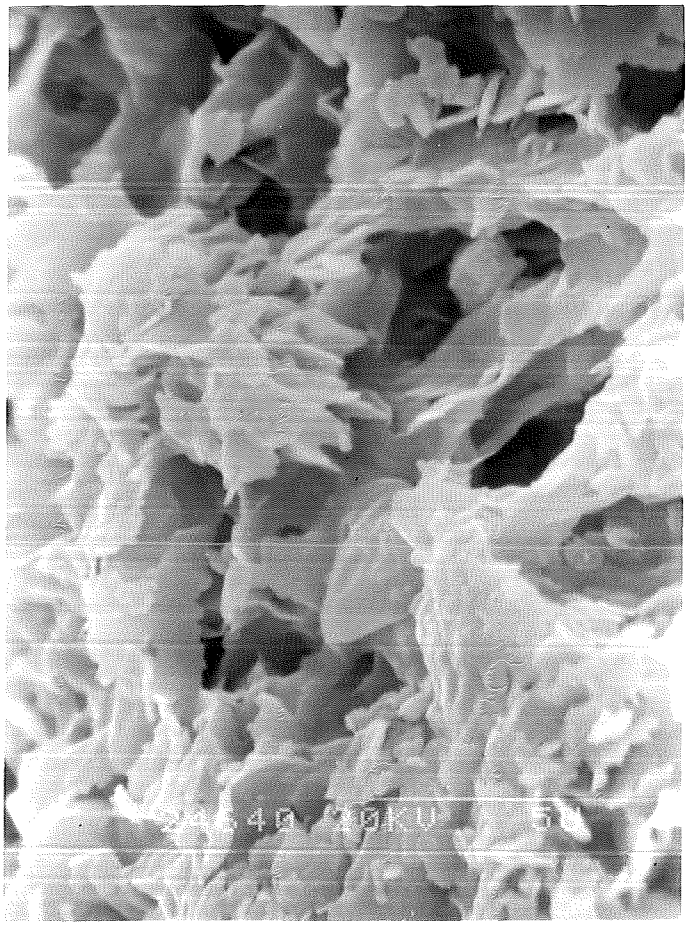

E

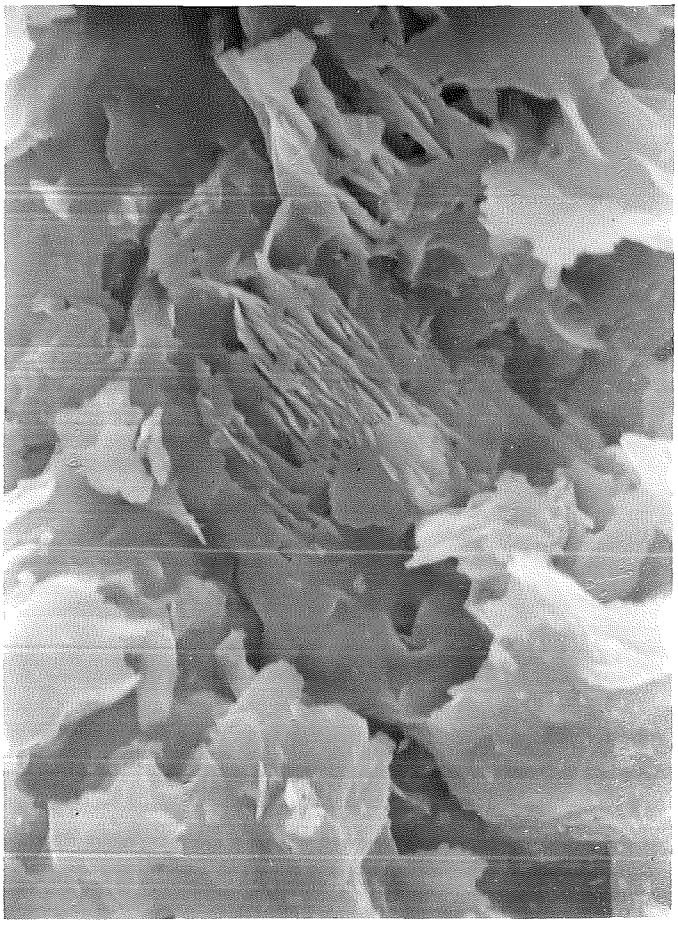

F

SAMPLE 560

A. General view of fabric of euhedral pyrite. Pyrite has commonly a cubic habit with mixed-layer clay matrix material between cubes. X-130

B. Detail of fabric of mixed-layer illite-smectite which commonly occurs between pyrite cubes. Pyrite in this sample constitutes less than 5% of the total rock, and occurs in either veinlets or as small disseminated cubes. X-660

C. General view of sandy tuff composed mostly of quartz and feldspar grains. Little effective porosity or permeability is available due to the fine-grained matrix material welding individual particles together. Elemental x-ray analysis indicates Al, Si, K, and Fe, and the principal cations. X-72

D. Detail of fabric of illite clay coating and projecting from various grain surfaces (arrows). Note the lack of effective porosity. Hydrothermal fluids would find this interval quite impermeable. X-1400

SAMPLE 560

E. Overview of fabric of rhyolitic tuff showing little textural variation. The finely crystalline, welded nature of the sample lacks any effective porosity, and permeability would more likely be controlled by large, well-connected fracture systems. X-150

F. Detail of fabric of an altered feldspar producing a vermicular clay-like structure. The stacked platelets have high Al, Si and K peaks on the EDAX. Tentatively could be called kaolinite, but other data (XRD or thin section analysis) would be required. X-3000

SAMPLE 360

A. General view of fabric and texture of rhyolitic tuff showing its overall fine-grained nature. Energy dispersive x-ray analysis indicates Al, Si, K, Ca and Fe are the principal cations of the sample. Much of the sample could be altered to an illite. X-72

B. Detail of fabric of the tuff's surface enriched in silica. Note its fine-grained appearance which lacks any effective porosity and permeability. X-720

E

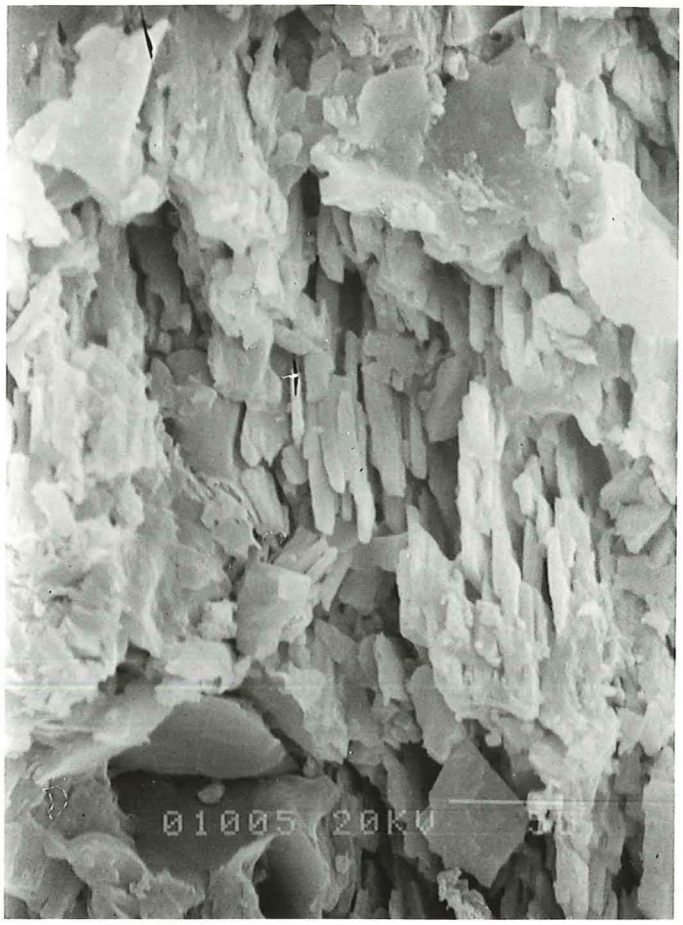

F

A

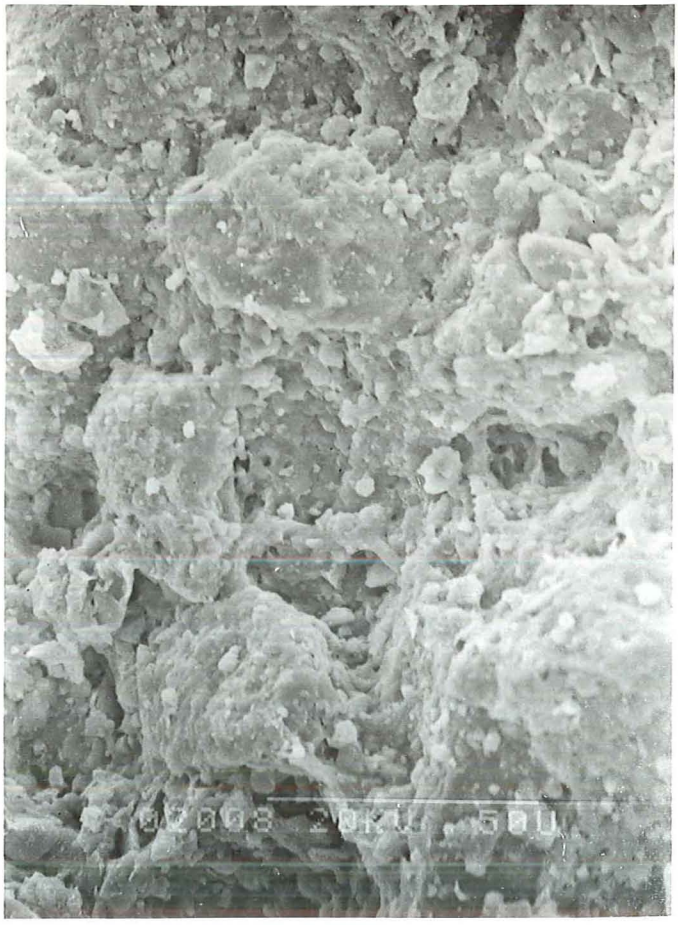

B

SAMPLE 360

C. Detail of fabric of layered kaolinite (K) showing discrete planes. Some of the hand samples viewed do contain biotite, and its presence in SEM samples seems likely.
X-1500

D. General view of fabric of illitic clay showing discrete bridges across microporosity. Note the lack of effective porosity and permeability. Most microporosity is poorly interconnected and, therefore, less effective for holding or passing hydrothermal fluids through.
X-300

E. Detail of fabric of clay bridges (arrows) which emanate from discrete grains or crystal boundaries. Clay is probably illite-rich smectite and would likely swell upon hydration of interlayer cations. X-750

F. Detail of fabric of possible kaolinite altering to fibrous illite. Elemental analysis shows the kaolinite in question (arrows) to contain a high amount of potassium. Note here the pseudo-vermicular structure of the clay.
X-3000

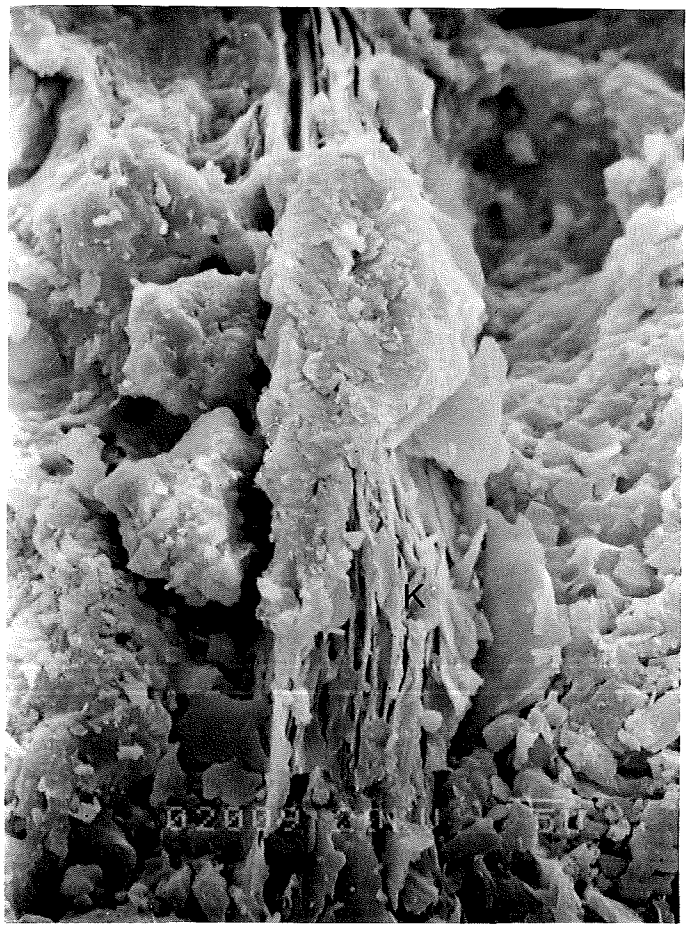

C

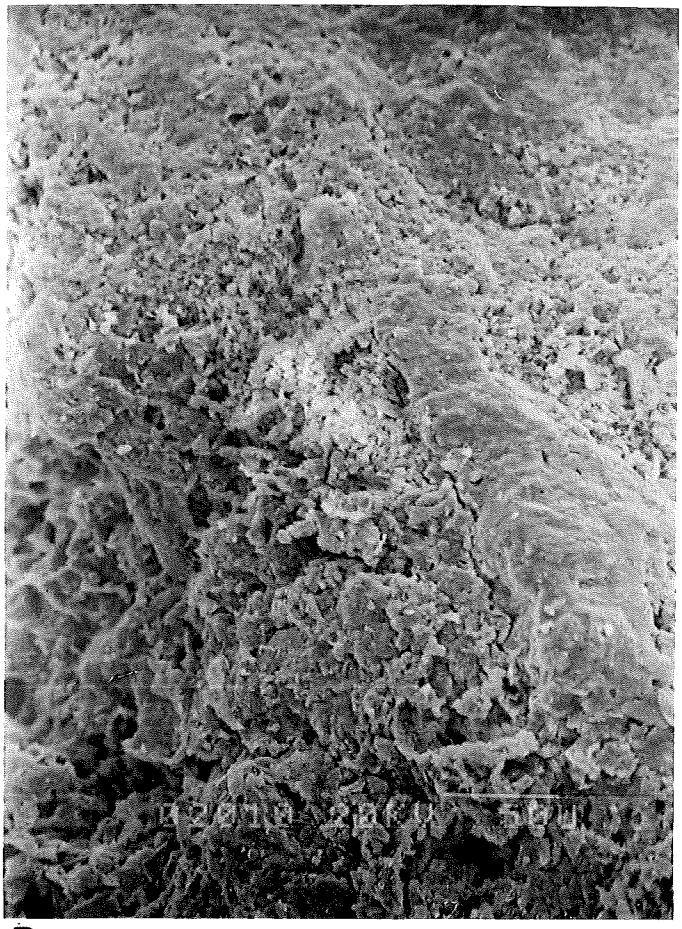

D

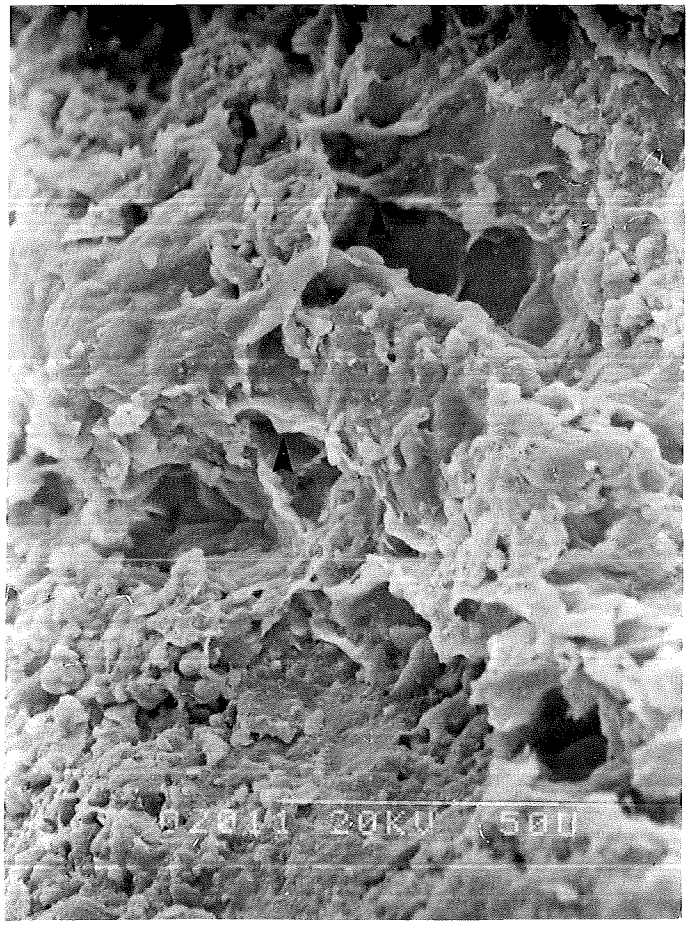

E

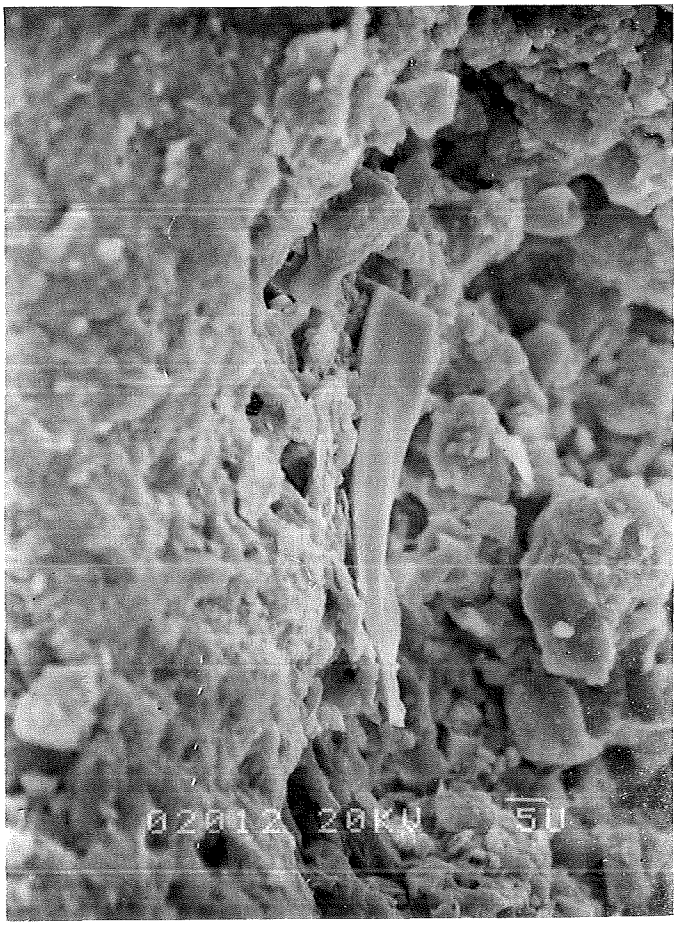

F

REFERENCES

Hulen, J.B. and Nielson, D.L., 1983, Stratigraphy of the Bandelier Tuff and characterization of high-level clay alteration in borehole B-20, Redondo Creek Area, Valles Caldera, New Mexico: Geoth. Resources Council, Trans., vol. 7, p. 163-168.

Hulen, J.B. and Nielson, D.L., 1982, Stratigraphic permeability in the Baca geothermal system, Redondo Creek area, Valles Caldera, New Mexico: Geoth. Resources Council, Trans., vol. 6, p. 27-30.

Smith, R.L., and Bailey, R.A., 1968, Resurgent cauldrons in Coats, R.R., Hay, R.L., and Anderson, C.H., eds., Studies in volcanology: Geol. Soc., America mem. 116, p. 613-662.